ARCHIVES OF ELECTRICAL ENGINEERING VOL. 66(4), pp. 815-828 (2017)

DOI 10.1515/aee-2017-0062

Torque characteristics of double-stator permanent magnet synchronous machines

CHUKWUEMEKA CHIJIOKE AWAH, OGBONNAYA INYA OKORO

Michael Okpara University of Agriculture
Umudike, Nigeria
e-mail: awahchukwuemeka@gmail.com, profogbonnayaokoro@ieee.org

(Received: 17.06.2017, revised: 10.09.2017)

Abstract: The torque profile of a double-stator permanent magnet (PM) synchronous machine of 90 mm stator diameter having different rotor pole numbers as well as dual excitation is investigated in this paper. The analysis includes a comparative study of the machine's torque and power-speed curves, static torque and inductance characteristics, losses and unbalanced magnetic force. The most promising flux-weakening potential is revealed in 13- and 7-rotor pole machines. Moreover, the machines having different rotor/stator (*Nr*/*Ns*) pole combinations of the form $Nr = Ns \pm 1$ have balanced and symmetric static torque waveforms variation with the rotor position in contrast to the machines having $Nr = Ns \pm 2$. Further, the inductance results of the analyzed machines reveal that the machines with odd rotor pole numbers have better fault-tolerant capability than their even rotor pole equivalents. A prototype of the developed double-stator machine having a 13-pole rotor is manufactured and tested for verification.

Key words: fault-tolerance, mutual-and self-inductance, power, static torque and torque-density

1. Introduction

A double-stator permanent magnet machine having a modulating ring, combines the advantages of magnetic-geared machines and that of traditional PM synchronous machines in one integrated system. This merits include but are not limited to a high torque/power density, better efficiency, good thermal dissipation capability owing to the stator-mounted PMs, a wide operating speed range, little maintenance, and a high reliability, etc. [1] and [2]. However, the high cost of magnets is still a global issue for electrical machine experts. Hence, a good number of researchers have developed improved machine topologies that are free of rare-earth magnets, yet with competitive performance as detailed in [3] and [4].

The obtainable flux-focusing potential in flux-switching PM machines which is noted in [5] is employed in this study to have the capability of maximizing the output torque. Moreover, an exhaustive study on different topologies of electric machines ranging from its merits and demerits to their unique characteristics are also given in [5]. Similarly, a precise account

of recent developments on flux-switching PM machines is given in [6] with their various features.

Furthermore, an improved torque density of a flux-switching PM machine having multiple stator teeth configuration is developed and analyzed in [7] using both two- and three-dimensional FEA approach in additional to a valid test result of the fabricated prototype machine. However, the investigated machine in [7] saturates quicker than the traditional flux-switching PM machine on overload condition. Similarly, the impact of design parameters on the overall performance of the flux-switching permanent magnet machine, which clearly shows that the output of the machine is dependent upon its structural geometries is presented in [8]. Similarly, the feasible stator and rotor pole combinations of the flux-switching PM machine is detailed in [9] in addition to quantitative comparison of the effects of its rotor pole number and winding topology to its electromagnetic performance. Also, a comparative study of different optimization techniques on the geometric dimensions of the flux-switching PM machine is presented by Zhu in [10]. The studies in [10], recommends the use of global optimization techniques using a genetic algorithm approach in place of a conventional step-by-step parametric optimization method.

The state-of-art of the different kinds of flux-switching machines is presented in [11]. Moreover, the condition to realize symmetrically induced electromagnetic force waveforms is also established in [11]. A new type of a flux-switching PM machine having an E-core stator structure with an enhanced torque capability and reduced magnet size is proposed and analyzed in [12], with valid experimental results. Furthermore, a novel hybrid flux-switching PM machine which uses both direct current and alternating current sources simultaneously is introduced in [13], in order to enhance its flux regulation and control.

Although the switched flux PM machines have high inherent magnetic isolation amongst its phases, which increases its reliability potentials; many authors have proposed different flux-switching machine topologies with improved fault-tolerance, in addition to enhanced torque density capabilities, as reported in [14], and [15]. Furthermore, a novel, doubly salient PM machine having an external mounted PM rotor and capable of delivering a high output torque as well as improved efficiency when compared to a conventional interior permanent magnet (IPM) machine of the same size is proposed and compared in [16].

It is worth mentioning that, the flux-switching PM machine exhibits good thermal and flux-weakening potentials compared to most of the other permanent magnet synchronous machines, although it could be easier demagnetized than the interior permanent magnet machine as noted in [17] from the in-depth comparison of different kinds of permanent magnet machines. Note also that, it is cost-sensitive to use ferrite magnets in place of high-energy density rare earth magnets, in particular on flux-switching PM machines; however adequate precaution must be taken during the design stage to avoid resultant demagnetization issues [17].

Magnetically-geared machines which artfully combines the advantages of magnetic gears and that of PM machines are good alternatives for direct-drive applications. Basically, these machines utilize the gearing effect of modulated magnetic fields in generating a high torque; in most cases, at a low operating speed. Quite a good number of investigations have been validated on the subject of magnetically-geared machines, as evidenced in [18] and [19]. How-

ever, this type of machine have complicated manufacturing issues owing to their complex structures. Further, a highly efficient, magnetically-geared PM machine with reduced PM volume is proposed in [20], by adopting a consequent pole configuration. It is verified in [21], that the style and placement of PMs on the stator of modulated PM machines are important in determining their overall performance; here a V-shaped mounted PM is proven to generate an output torque of about 38% higher than their equivalent I-shaped and rectangular mounted PMs.

In this paper, doubly-excited synchronous PM machines having doubly-salient and identical dual stator structures are analyzed. A comparative study of the machines with different pole numbers is also given. The sections in this paper are: introduction, torque characteristics, inductance profile, losses, efficiency and unbalanced magnetic force, experimental verification and conclusion. The two-dimensional finite element analysis (FEA) approach is employed in this study. Since the developed machines have separate inner- and outer-stator windings, it could be operated independently in safety applications. The developed machine in this study, resembles the one proposed in [22]; however with great disparity in their structural geometry and has an opposite operating principle. Similarly, the outer stator of the developed machine in this paper is similar to the one of an axially joined dual stator of the machine given in [23]. Nevertheless, their physical stator and rotor arrangements/structures are entirely different. The developed machine topology is shown in Fig. 1.

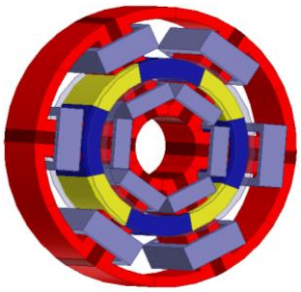

Fig. 1. 3D-structure of the analyzed double-stator PM machine

2. Torque characteristics

The predicted electromagnetic torque, T, of the analysed machine is expresssed as a function of fluxlinkage and inductances in Equation (1).

$$T = 1.5N_r[\psi_{PM} I_q + (L_d - L_q) I_d I_q], \tag{1}$$

where: N_r is the number of rotor poles, ψ_{PM} is the PM flux-linkage, I_d, I_q and L_d, L_q are the direct and quadrature-axis currents and inductances, respectively [5].

The radial air-gap flux densities of the analyzed machines on open-circuit condition is shown in Fig. 2. It could be seen that, the developed machines have similar flux density waveforms with peak-to-peak values of about 2 T. Similarly, the flux line distributions as well as the flux density maps of the compared machines on no-load condition are displayed in

Figs. 3 and 4, respectively. It should be noted that, flux per pole decreases as the pole number of the machines increases. Moreover, visible magnetic saturations are seen on the inner and outer stator teeth of the machines compared to other parts of the machines, likely due to their proximity to air-gap magnetic fields.

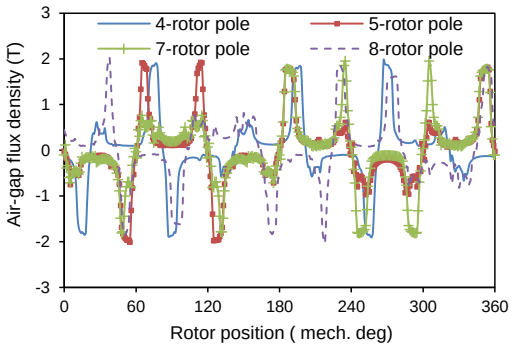

Fig. 2. Comparison of the air-gap flux densities of the developed machines

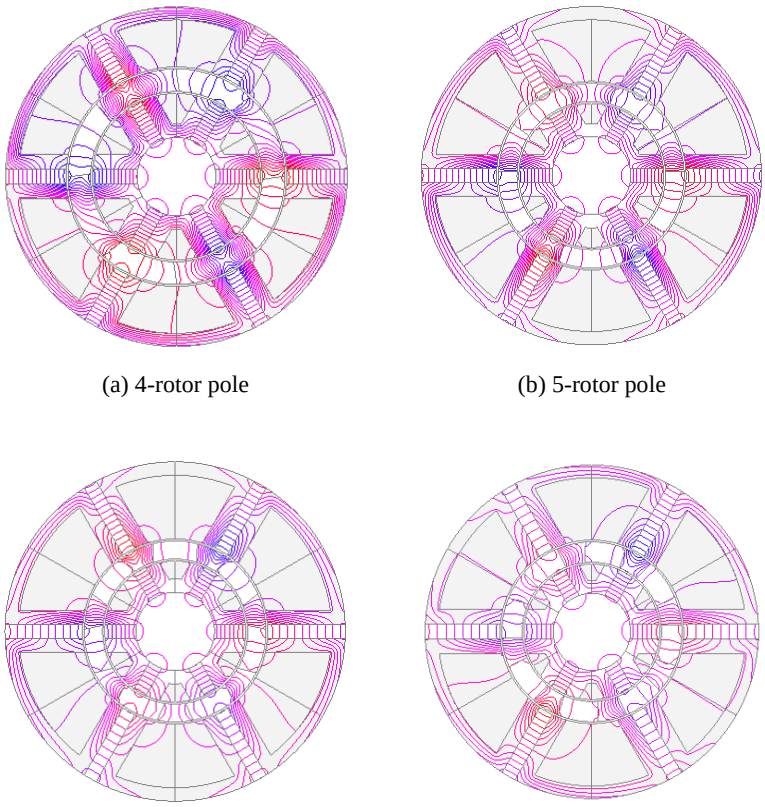

(a) 4-rotor pole (b) 5-rotor pole

(c) 7-rotor pole (d) 8-rotor pole

Fig. 3. Open circuit field distributions of analyzed machines at *d*-axis rotor position

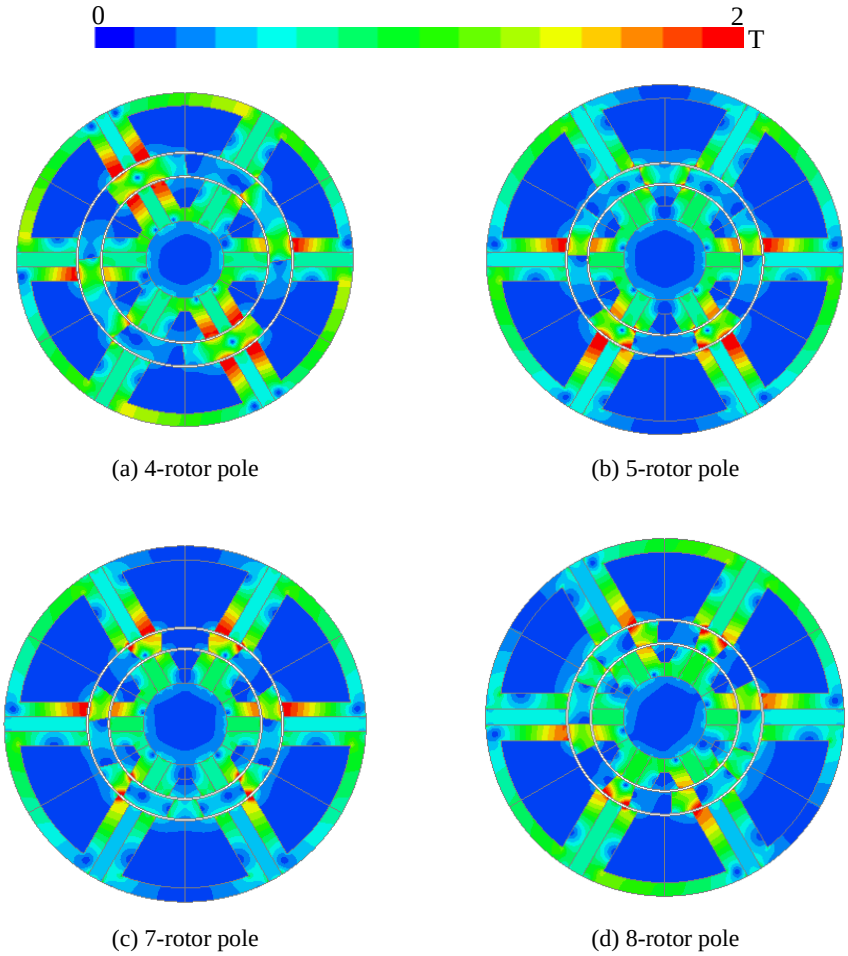

(a) 4-rotor pole (b) 5-rotor pole

(c) 7-rotor pole (d) 8-rotor pole

Fig. 4. Open circuit flux densities of the analyzed machines at *d*-axis rotor position

The static torque variations of the machines with rotor position are shown in Fig. 5. The results show that, the machines having odd rotor pole numbers have balanced and symmetrical static torque waveforms unlike their even rotor pole counterparts, whose static torque waveforms are both asymmetric and unbalanced in relations to the rotor position. Also, it is observed that, the waveforms are sensitive to load, with positive rise on increasing current. The predicted static torque is obtained by injecting direct-current (*DC*) to the three-phase windings of the machine using a star-connection technique such that the inputted phase B and phase C currents are equivalent to negative half of the current flowing in the phase A winding, i.e.:

$$I_a = I\,, \tag{2}$$

$$I_b = I_c = -0.5I\,, \tag{3}$$

where: I_a, I_b, and I_c are the phase A, B and C currents, I is the magnitude of the applied DC current.

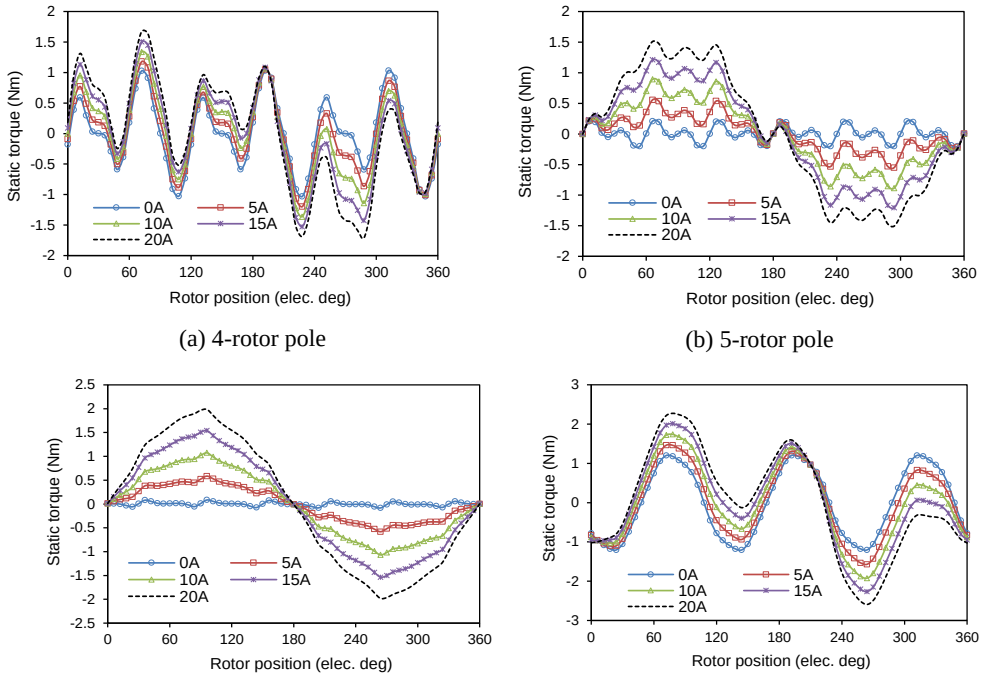

(a) 4-rotor pole

(b) 5-rotor pole

(c) 7-rotor pole

(d) 8-rotor pole

Fig. 5. Variation of static torque with rotor position, $I_a = I$ (A), and $I_b = I_c = -0.5I$ (A)

The torque-speed and power-speed envelops of the analyzed machines over the whole speed range are shown in Figs. 6 and 7. The computation was conducted at the maximum current and at a voltage of 15 A and of 22.9 V, respectively.

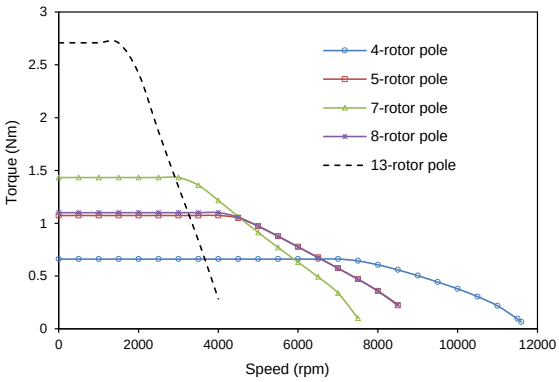

Fig. 6. Comparison of torque-speed characteristics, (V_{dc} = 22.9 V, I_{max} = 15 A)

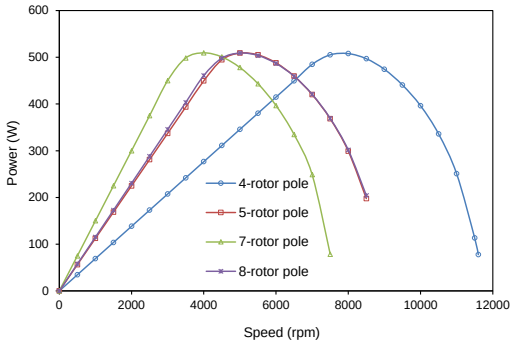

Fig. 7. Comparison of power-speed characteristics, (V_{dc} = 22.9 V, I_{max} = 15 A)

3. Inductance profile

The self- and mutual-inductances of the developed machines are depicted in Figs. 8 and 9, respectively. It should be noted that, the self-inductances of the analyzed machines are essentially similar in magnitude, except for their varying shapes on rotor positions.

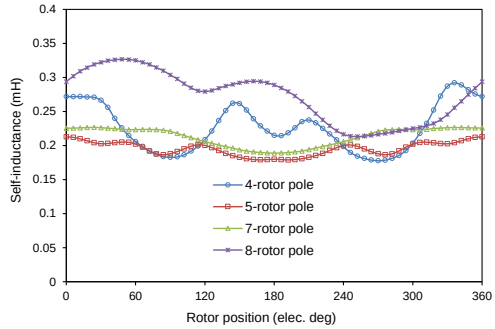

Fig. 8. Comparison of self-inductance with rotor position, I = 15 A

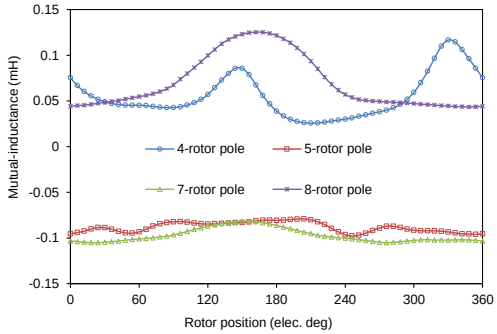

Fig. 9. Comparison of mutual-inductance with rotor position, I = 15 A

Similarly, the mutual-inductance of the machines having $N_r = N_s \pm 1$ and $N_r = N_s \pm 2$ have negative and positive values, respectively. Moreover, the low value of the mutual inductance seen in the odd-rotor pole machines indicates that they are more suited for fault-tolerant applications, since they have a relatively very low magnetic coupling between their phases as

pointed by [24]. Further, the values of direct- and quadrature-axis inductances of the machines are listed in Table 1. Note also that, the developed machines have negligible reluctance torque as seen from their near unity saliency ratios, since their *d*- and *q*-axis inductances are similar in magnitude as seen in Table 1.The computed self- and mutual-inductances are represented by Equations (4) and (5), respectively.

$$L_{aa} = (\psi_{aa} - \psi_{PM})/I\,, \tag{4}$$

$$M_{ab} = (\psi_{ab} - \psi_{PM})/I\,, \tag{5}$$

where: ψ_{aa} is the resultant flux-linkage in the phase A winding contributed by permanent magnets and the supplied phase A current, ψ_{ab} is the obtained flux-linkage in the phase A winding contributed by permanent magnets and currents from the phase B windings, ψ_{PM} is the no-load flux-linkage obtained from permanent magnets, I is the supplied current, L_{aa} and M_{ab} are the self- and mutual-inductances, respectively.

Moreover, other performance index of the analyzed machines, ranging from torque density, flux-weakening potential to efficiency characteristics are listed in Table 1.

Table 1. Parameters of the analyzed machines

Parameter	**Value**			
Rotor pole number, N_r	4	5	7	8
D-axis inductance, *Ld* (mH)	0.181	0.317	0.341	0.204
Q-axis inductance, *Lq* (mH)	0.241	0.303	0.340	0.210
Saliency ratio, *Lq* /*Ld*	1.33	0.96	0.997	1.03
PM flux (mWb)	7.41	9.63	9.27	6.15
Kfw	0.37	0.49	0.55	0.49
Base speed (rpm)	6800	4100	3000	3900
Maximum speed (rpm)	11600	8800	7500	8900
Maximum speed/base speed	1.7	2.15	2.5	2.28
Maximum torque (N·m)	0.66	1.07	1.43	1.10
Maximum power (W)	507.80	508.97	509.42	509.03
Self-inductance, L_{aa} (mH)	0.226	0.195	0.213	0.273
Mutual-inductance, M_{ab} (mH)	0.06	–0.09	–0.097	0.07
Mab/Laa	0.2655	–0.462	–0.455	0.256
Torque density (kN·m/m^3)	8.49	14.54	19.12	14.31
Efficiency (%)	88.49	93.58	93.48	90.25

4. Losses, efficiency and unbalanced magnetic force

The FEA predicted stator and rotor losses in this study are calculated using the classical Steinmetz loss equation given in (6). It should be noted that, the rotational losses such as the

windage loss and frictional loss in the bearings are neglected in this study since we employed the time-stepping 2D-FEA approach instead of the 3D-FEA due to time-constraint. However, the mechanical output power of the analyzed machine is calculated as a function of the rotational speed, N (rad/sec) and the average electromagnetic torque, T (N·m) as seen in Equation (7) under a fixed copper loss condition of 30 W. Moreover, the FEA predicted eddy current losses in the magnets of the investigated machine at varying speed is shown in Fig. 10a. The PM eddy current loss in the analyzed double-stator flux-switching PM machine could be mitigated by adopting the recommended magnet segmentation method proposed in [25]. Similarly, the comparison of the total core losses consisting of both the stator core and rotor core losses of the analyzed machines are depicted in Fig. 10b. Further, a comparison of the predicted losses at a rated current of 15 A and a rotor speed of 4000 rpm, respectively is shown in Fig. 11.

Furthermore, the FEA predicted values of the efficiencies at different rotor speed are enumerated in Table 2.

$$P_{\text{loss}} = K_h B_m^2 f + K_e (B_m f)^{1.5} + K_c (B_m f)^2 , \tag{6}$$

where: B_m is the maximum value of the magnetic flux density, f is the frequency, K_h, K_e, and K_c are the loss coefficients for hysteresis, excess and eddy current losses, respectively.
Similarly, the efficiency of the machine is given as:

$$\eta = \frac{P_{\text{out}}}{P_{\text{out}} + \text{losses}} = \frac{2\pi NT}{(2\pi NT) + P_{\text{copper}} + P_{\text{core}} + P_{\text{magnet}}} 100\% , \tag{7}$$

where: P_{out} is the mechanical output (W), T is the average torque (N·m), N is the rotational speed (rad/s), P_{core}, P_{magnet} and P_{copper} are the total core loss, PM eddy current loss and copper loss, respectively.

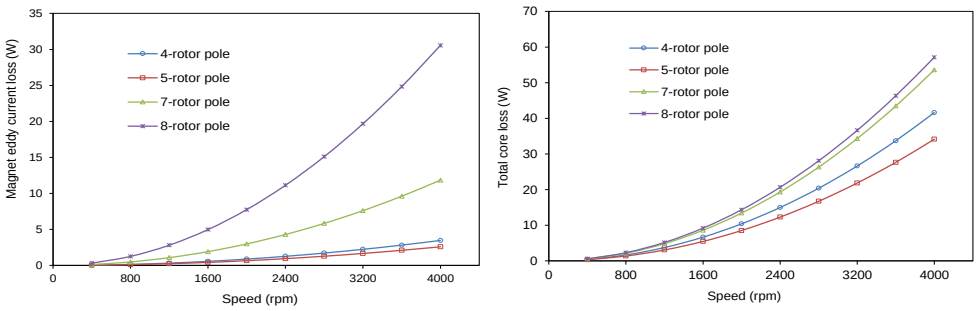

(a) Permanent magnet eddy current loss (b) Total core loss

Fig. 10. Variation of losses with rotor speed, copper loss = 30 W

The plots of unbalanced magnetic force (UMF) in both *x*- and *y*-axis directions on the rotor as well as the magnitude of its UMF variation over different rotor positions is displayed in Figs. 12 and 13, respectively. It is obvious from Figs. 12 and 13 that, the developed machines

having the odd-number of rotor poles exhibit large unbalanced magnetic force (UMF) on the rotor. This UMF effect is significantly high in the compared 5-rotor pole and 7-rotor pole machines compared to the ones of higher rotor poles.

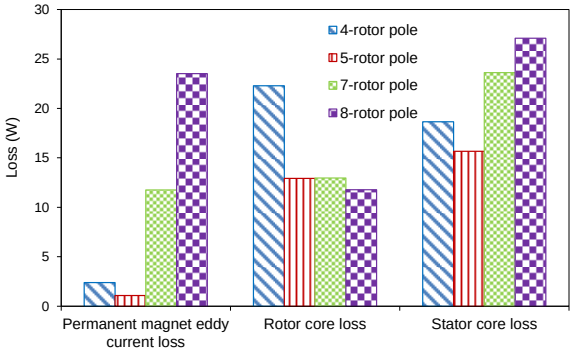

Fig. 11. Comparison of losses at 4000 rpm, current = 15 A

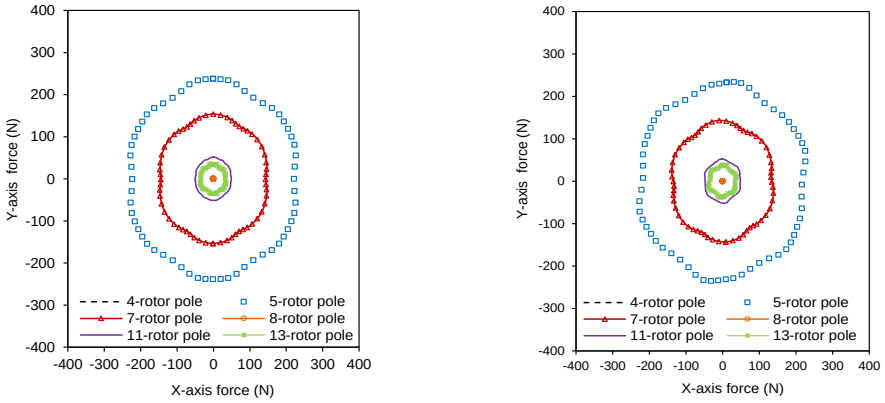

(a) 0 A (b) 10 A

Fig. 12. Variation of unbalanced magnetic force

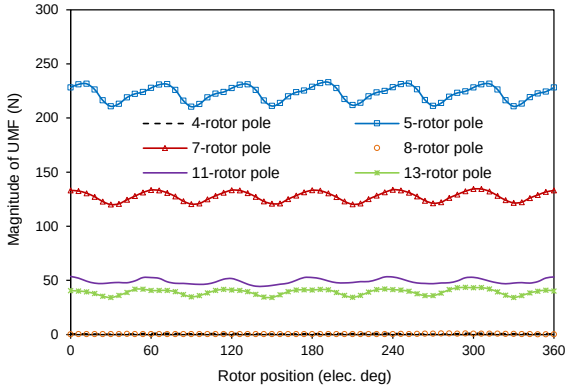

Fig. 13. Comparison of unbalanced magnetic force, current = 15 A

Table 2. FEA values of efficiency at different speed

Speed (rpm)	Efficiency			
	4-rotor pole	**5-rotor pole**	**7-rotor pole**	**8-rotor pole**
400	65.00	76.13	80.60	75.53
800	78.05	86.02	88.65	85.04
1200	83.28	89.72	91.41	88.28
1600	85.87	91.52	92.63	89.62
2000	87.26	92.51	93.21	90.15
2400	88.01	93.08	93.44	90.25
2800	88.37	93.39	93.48	90.12
3200	88.49	93.54	93.40	89.83
3600	88.44	93.58	93.24	89.45
4000	88.28	93.55	93.03	89.01

Further, [26] clearly pointed out that unbalanced magnetic force will act on the rotor of a given electric machine whose stator and rotor poles have an integer difference of 1, due to the eccentric nature of the rotor of such machine configuration in addition to its asymmetric magnetic features. Further analysis on the UMF effect resulting from rotor eccentricity is investigated and confirmed in [27].

5. Test results

The fabricated double-stator PM machine is shown in Fig. 14, which consists of the assembled inner and outer stators, in addition to the 13-pole cup-rotor modulating steel ring. In order to save cost, we manufactured one prototype having a 13-rotor pole, since an extended study shows that it has the best torque performance as depicted in Fig. 6.

The experimental set-up of the prototype machine for the static test measurements is shown in Fig. 14c. The measured values of the induced electromotive force are displayed in Fig. 15. Similarly, the static torque waveforms of the measured results are compared with the predicted FEA results in Fig. 16 showing good match. An error difference of about 12% is recorded between the measured and predicted static torque results, due to manufacturing imperfections.

6. Conclusions

Torque performance of double-stator PM machines having dual excitations as well as doubly-salient stator structures with particular reference to their varying rotor pole numbers are investigated.

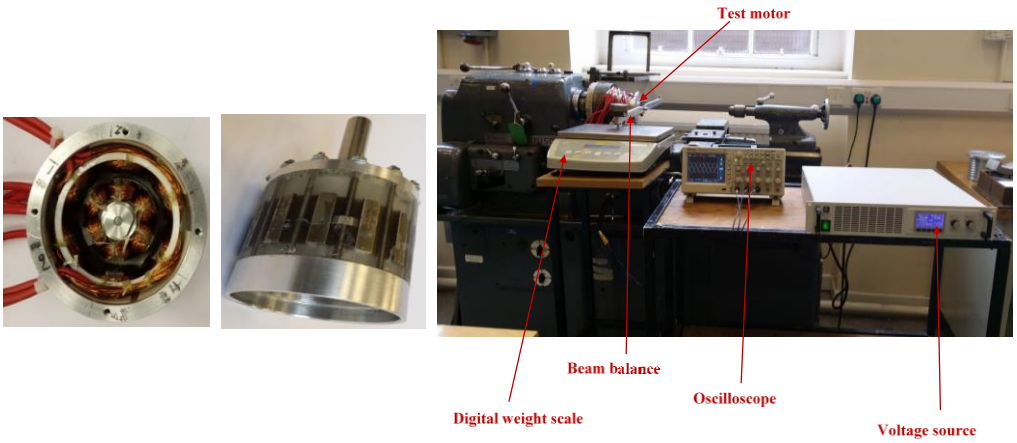

(a) Coupled inner and outer stator (b) 13-pole rotor (c) Test rig of the prototype

Fig. 14. Manufactured double-stator PM machine

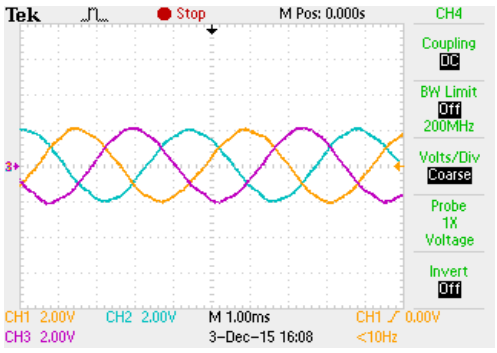

(a) Inner stator back-EMF

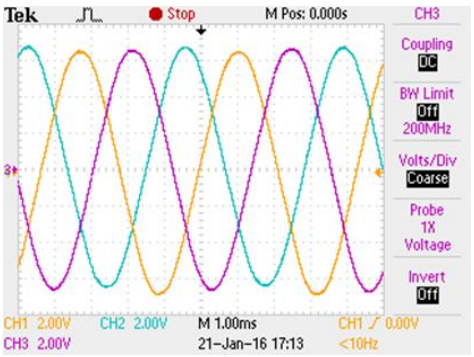

(b) Outer stator back-EMF

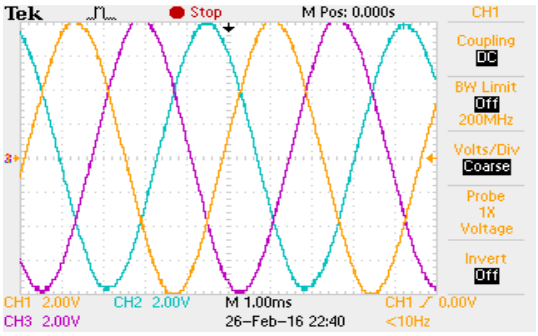

(c) Total back-EMF of series connected inner and outer stators

Fig. 15. Tested back-EMF results of the prototype, 2 V/div, at 400 rpm

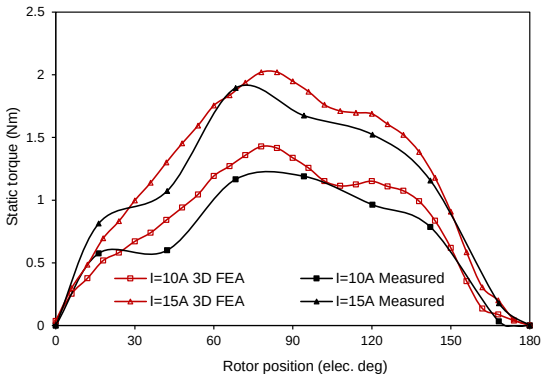

Fig. 16. Comparison of static torque with different load current of the prototype (I_a = -2I_b = -2I_c)

The analysis shows that the 13- and 7-rotor pole machines have the best flux-weakening potential amongst the analyzed machines, due to their higher ratio of maximum speed to base speed value and a high flux-weakening factor; this is quite desirable in traction applications. Furthermore, it is observed that the odd-rotor pole machines are the most suitable candidates for fault-tolerant applications, owing to their very low magnetic coupling and reasonable self-inductance values. The analyses are validated by experiments with agreeable results.

References

[1] Boldea I., Tutelea L.N., Parsa L., Dorrell D., *Automotive electric propulsion systems with reduced or no permanent magnets: an overview*, IEEE Transactions on Industrial Electronics, vol. 61, no. 10, pp. 5696-5711 (2014).

[2] Yang Z., Shang F., Brown I.P., Krishnamurthy, M., *Comparative study of interior permanent magnet, induction, and switched reluctance motor drives for EV and HEV applications*, IEEE Transaction on Transportation Electrification, vol. 1, no. 3, pp. 245-254 (2015).

[3] Chiba A., Kiyota K., Hoshi N., Takemoto M., Ogasawara S., *Development of a rare-earth-free SR motor with high torque density for hybrid vehicles*, IEEE Transactions on Energy Conversion, vol. 30, no. 1, pp. 175-182 (2015).

[4] Lee C.H.T., Chau K.T., Liu C., Ching T.W., Li F., *Mechanical offset for torque ripple reduction for magnetless double stator doubly salient machine*, IEEE Transactions on Magnetics, vol. 50, no. 11, art. seq. no. 8103304 (2014).

[5] Zhu Z.Q., Howe D., *Electrical machines and drives for electric, hybrid, and fuel cell vehicles*, Proceedings of the IEEE. vol. 95, no. 4, pp. 746-765 (2007).

[6] Zhu Z.Q., *Switched flux permanent magnet machines-Innovation continues*, Proceedings of International Conference on Electrical Machines and Systems, Beijing, P.R., pp. 1-10 (2011).

[7] Zhu Z.Q., Chen J.T., Pang Y., Howe D., Iwasaki S., Deodhar R., *Analysis of a novel multi-tooth flux-switching PM brushless AC machine for high torque direct-drive applications*, IEEE Transactions on Magnetics, vol. 44, no. 11, pp. 4313-4316 (2008).

[8] Chen J.T., Zhu Z.Q., Iwasaki S., Deodhar R.P., *Influence of slot opening on optimal stator and rotor pole combination and electromagnetic performance of switched-flux PM brushless AC machines*, *IEEE Transactions on Industry Applications*, vol. 47, no. 4, pp. 1681-1691 (2011).

[9] Chen J.T., Zhu Z.Q., *Winding configurations and optimal stator and rotor pole combination of flux switching PM brushless AC machines*, IEEE Transactions on Energy Conversion, vol. 25, no. 2, pp. 293-302 (2010).

[10] Zhu Z.Q., Liu X., *Individual and global optimization of switched flux permanent magnet motors*, Proceedings of Intern. Conf. on Electrical Machines and Systems, Beijing, P.R., pp. 1-10 (2011).

[11] Zhu Z.Q., Chen J.T., *Advanced flux-switching permanent magnet brushless machines*, IEEE Transactions on Magnetics, vol. 46, no. 6, pp.1447-1453 (2010).
[12] Chen J.T., Zhu Z.Q., Iwasaki S., Deodhar R.P., *A novel E-core switched flux PM brushless AC machine*, IEEE Transactions on Industry Applications, vol. 47, no. 3, pp. 1273-1282 (2011).
[13] Chen J.T., Zhu Z.Q., Iwasaki S., Deodhar, R.P., *A novel hybrid-excited switched-flux brushless AC machine for EV/HEV applications*, IEEE Transactions on Magnetics. vol. 60, no. 4, pp. 1365-1373 (2011).
[14] Xue X., Zhao W., Zhu J., Liu G., Zhu X., Cheng M., *Design of five-phase modular flux-switching permanent-magnet machines for high reliability applications*, IEEE Transactions on Magnetics, vol. 49, no. 7, pp. 3941-3944, (2013).
[15] Hua W., Yin X., Zhang G., Cheng M., *Analysis of two novel five-phase hybrid-excitation flux-switching machines for electric vehicles*, IEEE Transactions on Magnetics. vol. 50, no. 11, art. seq. no. 700305 (2014).
[16] Gu L., Wang W., Fahimi B., Kiani M., *A novel high energy density double salient exterior rotor permanent magnet machine*, IEEE Transactions on Magnetics, vol. 51, no. 3, art. seq. no. 8102604 (2015).
[17] Fasolo A., Alberti L., Bianchi N., *Performance comparison between switching-flux and IPM machines with rare-earth and ferrite PMs*, IEEE Transactions on Industry Applications, vol. 50, no. 6, pp. 3708-3716 (2014).
[18] Liu C.T., Chung H.Y., Hwang C.C., *Design assessments of a magnetic-geared double-rotor permanent magnet generator*, IEEE Transactions on Magnetics, vol. 50, no. 1, art. seq. no. 4001004 (2014).
[19] Zhang X., Liu X., Chen Z., *A novel coaxial magnetic gear and its integration with permanent-magnet brushless motor*, IEEE Transactions on Magnetics, vol. 52, no. 7, art. seq. no. 8203304 (2016).
[20] Bai J., Zheng P., Yu B., Cheng L., Zhang S., Liu Z., *Investigation of a magnetic-field modulated brushless double-rotor machine with the same polarity of PM rotor*, IEEE Transactions on Magnetics, vol. 51, no. 11, art. seq. no 8110004 (2015).
[21] Fukami T., Ueno Y., Shima K., *Magnet arrangement in novel flux-modulating synchronous machines with permanent magnet excitation*, IEEE Transactions on Magnetics, vol. 51, no. 11, art. seq. no. 8206104 (2015).
[22] Yunyun C., Li Q., Xiaoyong Z., Hua W., Wang Z., *Electromagnetic performance analysis of double-rotor stator permanent magnet motor for hybrid electric vehicle*, IEEE Transactions on Magnetics, vol. 48, no. 11, pp. 4204-4207 (2012).
[23] Li Y., Bobba D., Sarlioglu B., *Design and performance characterization of a novel low-pole dual-stator flux-switching permanent magnet machine for traction application*, IEEE Transactions on Industry Applications, vol. 52, no. 5, pp. 4304-4314 (2016).
[24] Bianchi N., Bolognani S., Pre M.D., Grezzani G., *Design considerations for fractional-slot winding configurations of synchronous machines*, IEEE Transactions on Industry Applications, vol. 42, no. 4, pp. 997-1006 (2006).
[25] Zhu Z.Q., Pang Y., Chen J.T., Owen R.L., Howe D., Iwasaki S., Deodhar R., Pride A., *Analysis and reduction of magnet eddy current loss in flux-switching permanent magnet machines*, Proceedings of IET Conference on Power Electronics, Machines and Drives (PEMD), York, England, pp. 120-124 (2008).
[26] Zhu Z.Q., Ishak D., Howe D., Chen J.T., *Unbalanced magnetic force in permanent-magnet brushless machines with diametrically asymmetric phase windings*, IEEE Transactions on Industry Applications, vol. 43, no. 6, pp. 1544-1553 (2007).
[27] Mahmoud H., Bianchi N., *Eccentricity in synchronous reluctance motors – Part II: Different rotor geometry and stator windings*, IEEE Transactions on Energy Conversion, vol. 30, no. 2, pp. 754-760 (2015).